Colloids and Surfaces A 556 (2018) 284–290

Contents lists available at ScienceDirect

Colloids and Surfaces A

journal homepage: www.elsevier.com/locate/colsurfa

# Facile one-pot synthesis of wood based bismuth molybdate nano-eggshells with efficient visible-light photocatalytic activity

Yingying Li[a,b], Bin Hui[c], Likun Gao[a,b], Fenglong Li[a,b], Jian Li[a,b,*]

[a] Research Center of Wood Bionic Intelligent Science, Northeast Forestry University, Harbin 150040, China
[b] Key Laboratory of Bio-Based Material Science and Technology of Ministry of Education, Northeast Forestry University, Harbin 150040, China
[c] State Key Laboratory of Bio-Fibers and Eco-Textiles, Qingdao University, Qingdao 266071, China

## GRAPHICAL ABSTRACT

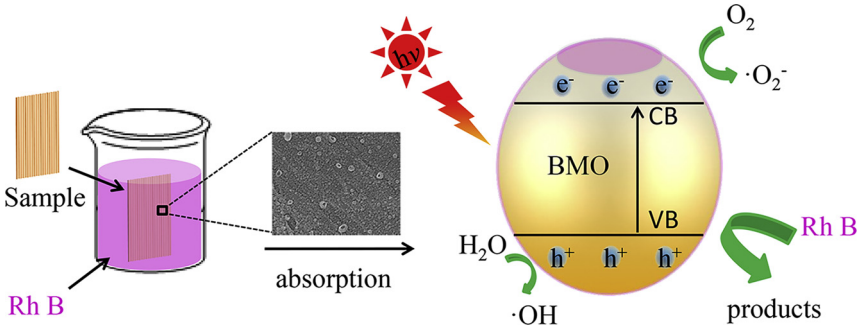


## ARTICLE INFO

*Keywords:*
Wood
Potocatalysis
Bismuth molybdate
One-pot synthesis

## ABSTRACT

Photocatalysis, which harnesses light to degrade pollutants, has been considered as the most green and low-cost approach for environmental remediation. In this work, a novel wood-based photocatalyst was prepared by a simple one-pot way. The as-prepared samples were characterized by X-ray diffraction, scanning electron microscopy, energy dispersive X-ray spectroscopy, UV–vis diffuse reflectance spectroscopy and X-ray photoelectron spectra, respectively. Results showed that the synthesized bismuth molybdate nano-eggshells were evenly grown on the surface of wood substrate. Additionally, its morphologies were strongly dependent on the initial pH of precursor solution and the presence of wood substrate. The photocatalytic activity of the samples was evaluated based on the decomposition of rhodamine B under visible light irradiation. The sample prepared at pH 6 showed superior performance for the photodegradation of rhodamine B, in comparison to the pure bismuth molybdate powders and the samples prepared at other pH value. The stability, photocatalytic mechanism and the reasons for improving photocatalytic activity were also discussed. This study offers exciting opportunities to achieve the industrialization of photocatalytic wood products.

## 1. Introduction

As a green technology, photocatalysis has been gathering increasing interest because it can be widely applied to many domains that offer an economic and ecologically safe option to solve energy and pollution problems [1–4]. A representative example is the photosynthesis of green plants, in which trees absorb carbon dioxide from the atmosphere under visible light in the photocatalytic process and store it in the plant

* Corresponding author at: Research Center of Wood Bionic Intelligent Science, Northeast Forestry University, Harbin 150040, China.
*E-mail address:* nefujianli@163.com (J. Li).

https://doi.org/10.1016/j.colsurfa.2018.08.041
Received 5 June 2018; Received in revised form 16 August 2018; Accepted 16 August 2018
Available online 18 August 2018
0927-7757/ 

tissues [5–8]. However, trees will lose their photocatalytic ability when they are processed into wood products. Nowadays, wooden products are extensively used in daily applications, such as buildings, bridges, furniture and indoor decorations [9]. Furthermore, due to the use of the non-renewable materials, the applications for wood increase significantly with the increasing concerns of population and sustainability. To meet market requirements and compete with other advanced materials, many attempts have been made to create new functions for wood [10–12]. Therefore, the future looks bright for functional wooden products with photocatalytic ability.

It is commonly known that wood has three major components which are cellulose, hemicellulose, and lignin. The network of the components and the space of parallel hollow tubes construct the multi-scale porous structure, which offers the penetrability, accessibility and reactivity of wood materials [13,14]. As a result, the unique composition and subtle hierarchical structures of wood lay the foundation for their further functionalization. In recent years, more and more attention has been forced on semiconductor photocatalytic materials such as $TiO_2$, ZnO and $ZrO_2$ due to their potential applications in environmental cleaning, solar energy utilization and hydrogen generation from water splitting [15–18]. Among them, bismuth-based compounds have attracted considerable attention for the strong visible light photocatalytic activities [19,20]. $Bi_2MoO_6$ with the layered bismuth oxide family is of special interest due to its dielectric, ion-conductive, luminescent and catalytic properties [21–23]. This was demonstrated in a number of studies that the nontoxic $Bi_2MoO_6$ could perform as an excellent photocatalyst and solar energy conversion material for pollutant degradation, water splitting and $CO_2$ reduction, due to its suitable band location and superior spectral properties [24–26].

There are several works investigated on the preparation and properties of titania-wood hybrid materials [27–30], and they found the hybrid photocatalyst shows great photocatalytic activity for organic degradation. However, to the best of our knowledge, there is no work focused on the preparation and photocatalytic properties of wood-based bismuth molybdate (W-BMO). To realize this goal, we propose a simple one-pot way to prepare W-BMO photocatalyst with eggshell structure. The fabricated W-BMO has good visible light responsive photocatalytic activity with the decomposition of rhodamine B (RhB). Its morphology, phase structure, chemical composition, optical properties, stability, photocatalytic mechanism and the reasons of improving photocatalytic activity were investigated.

## 2. Experimental

### 2.1. Materials

Wood slices (15 mm × 15 mm × 0.5 mm) of white poplar (Populus tomentosa Carr.) were used in this experiment. Bismuth nitrate ($Bi(NO_3)_3{\cdot}5H_2O$), sodium molybdate ($Na_2MoO_4{\cdot}2H_2O$), ethanol, ammonia, and rhodamine-B (RhB) was purchased from Shanghai Aladdin Biochemical Technology Co., Ltd. (Shanghai, China). Nitric acid ($HNO_3$) and sodium hydroxide (NaOH) were purchased from Shanghai Chemical Co. Ltd (Shanghai, China). The ethanol (99.5%) was purchased from Kaitong Chemical Reagent Co., Ltd (Tian jian, China). All of the chemicals were used as received without further purification.

### 2.2. Fabrication of W-BMO photocatalytic material

Four mmol $Bi(NO_3)_3{\cdot}5H_2O$ was dissolved in 40 mL nitric acid solution (4 mol/L) and stirred for several minutes. A total of 0.484 g of $Na_2MoO_4{\cdot}2H_2O$ was dissolved in 36 mL of deionized water. The white precipitate first appeared and then disappeared when the $Na_2MoO_4$ solution was dropwise added into the above mixed solution. The different pH value of the precursor suspension was adjusted with 2 mol/L NaOH solution under stirring, while amorphous white precipitate formed during this process. After being stirred for 3 h, the wood slice and the above solution were transferred into a 100 ml stainless steel autoclave. The autoclave was sealed and maintained at 140 °C for 12 h, and then cooled down to room temperature. Finally, the resulting samples were removed from the solution, washed with deionized water for several times and dried at 60 °C for over 24 h in vacuum. In this experiment, five samples with different pH value of 5, 6, 7, 8 and 9 were prepared, and they were defined as W-BMO-5, W-BMO-6, W-BMO-7, W-BMO-8 and W-BMO-9. It should be mention that the loading amount of bismuth molybdate on the W-BMO-6 was about 20 wt %. Besides, for the purpose of comparison, pure $Bi_2MoO_6$ was also prepared with the same method except that the wood slice was absent.

### 2.3. Characterization

The phase structure of the as-prepared products was checked by the X-ray diffraction measurements (XRD, Rigaku, and D/MAX 2200) operated with Cu target radiation ($\lambda$ = 1.54 Å). The UV–vis diffuse reflection spectra of the samples were recorded on a UV–vis spectrophotometer (UV–vis DRS, TU-1901, China) equipped with an integrated sphere attachment by using $BaSO_4$ as a reference. The surface morphologies and microstructures of as-prepared samples were analyzed by a field-emission scanning electron microscope (JEOL JSM-7500F). The surface components of the samples were determined via energy dispersive X-ray analysis (EDXA). X-ray photoelectron spectra (XPS) measurement was recorded on an ESCALAB 250Xi photoelectron spectrometer using Al *Kα* (1486.6 eV) radiation. Specific surface areas of the samples were measured by the Brunauer-Emmett-Teller (BET) method based on nitrogen adsorption at the liquid nitrogen temperature using a 3H-2000PS2 unit (Beishide Instrument S&T Co., Ltd). Photoluminescence (PL) spectra of the samples were taken with a FluoroMax-4 spectrophotometer.

### 2.4. Photocatalytic activity experiments

The photocatalytic performance of the samples was evaluated by the degradation of rhodamine B (RhB) under visible-light irradiation using a 500 W solar simulator (XES-40S2-CE, SAN-EI Electric) with a 420 nm cutoff filter. The samples were placed 15 cm away from the light source, and the experiments were carried out at room temperature. In each experiment, photocatalyst was added into 50 mL 10 mg/L of RhB. Before illumination, the solution was magnetically stirred in the dark for 3 h to establish adsorption/desorption equilibrium between the dye and the catalyst. At given irradiation time intervals, 3 ml of the solution was extracted and centrifuged to remove the potential impurities. The centrifuged solution was monitored with an UV–vis spectrophotometer in terms of the absorbance at 553 nm during the photodegradation process. An air conditioner was employed to maintain the temperature at 25 °C.

## 3. Results and discussion

### 3.1. Phase structures of samples

The formation of the as-prepared samples was well confirmed by XRD analysis. Fig. 1 presents the XRD patterns of the pristine wood and the W-BMO samples prepared at different pH values. The diffraction peaks centered at 16.1° and 22.2°, which correspond to the (101) and (002) diffraction planes of cellulose in wood substrate. After hydrothermal treatment, the above two peaks were almost the same and some new peaks appeared. As we can see, when the pH values in the reaction system were kept at 5 and 6, peaks centered at 10.8°, 28.0°, 31.9°, 32.5°, 46.2°, 46.6°, 54.9°, 55.4° and 57.7° were observed. These peaks match well with the crystal planes of $Bi_2MoO_6$ (JCPDS 21-0102). Additionally, as the sample prepared at pH 10, its diffraction peaks at 26.9°, 31.0°, 44.1°, 52.7° and 55.1° can be perfectly identified to (111), (200), (220), (311) and (222) crystal planes of $Bi_{3.64}Mo_{0.36}O_{6.55}$ (JCPDS 43-0446),